Supporting Information

to

Modeling Excluded Volume Effects for the Faithful Description of the Background Signal in Double Electron-Electron Resonance

Daniel R. Kattnig,[a] Jörg Reichenwallner,[b,c] and Dariush Hinderberger[b,c,*]

[a] Graz University of Technology, Stremayrgasse 9, 8010 Graz, Austria.
[b] Max Planck Institute for Polymer Research, Ackermannweg 10, 55128 Mainz, Germany.
[c] Martin-Luther-Universität Halle-Wittenberg, Institute of Chemistry, Von-Danckelmann-Platz 4, 06120 Halle (Saale), Germany
[*] dariush.hinderberger@chemie.uni-halle.de, phone: +345 55 25230, fax: +49 345 55 27576

Table S1: Tabulation of $\alpha(d)$ as defined in eq. (18) of the main manuscript. The non-equidistant grid of arguments has been chosen such that the function can be reproduced by cubic spline interpolation in the interval [0, 50] with an absolute error smaller than 10^{-4}. Typically, 17 significant decimal places are given allowing the lossless conversion to IEEE 754 double precision numbers.

d	$\alpha(d)$
0	0.00000000000000000
0.15625	0.05162706629556498
0.3125	0.10289575864793842
0.625	0.20297572751410472
0.9375	0.29768857369338311
1.25	0.38497223190865181
1.5625	0.46340692632428295
1.875	0.53227764081851469
2.1875	0.59154366480800064
2.5	0.64172880600106878
3.125	0.71877399707291740
3.75	0.77241540554356620
4.375	0.81056539532051426
5	0.83814761550748048
6.25	0.87152574963314597
6.875	0.88136170843399123
7.5	0.88929899054375268
8.125	0.89662337341543504
8.75	0.90375014193053403
10	0.91679121736453198
11.25	0.92715281382076650
12.5	0.93451470664197596
13.75	0.93970817029148796
15	0.94439511732196284
17.5	0.95297886136061277
18.75	0.95613625951642133
20	0.95858908097957250
21.25	0.96088237885312859
22.5	0.96318267190245481
25	0.96703857507138751
27.5	0.96982178852619641
30	0.97249562098761656
32.5	0.97453759156555443
35	0.97634932000970439
40	0.97928361985960965
45	0.98161658730029958
50	0.98348189110936179

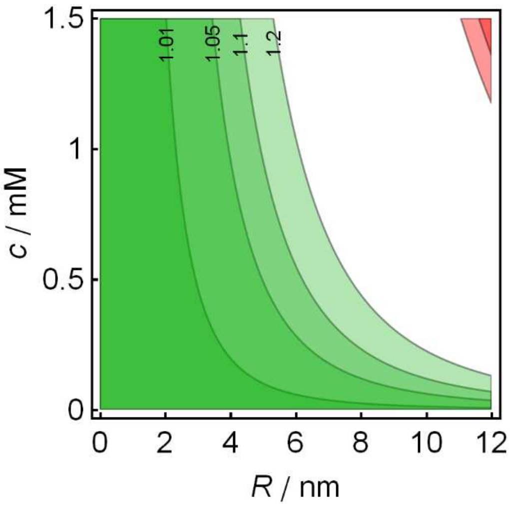

Figure S1: (R,c)-regions for which the Heaviside step function approximation of the pair-correlation function can be regarded as valid. The plot gives contours of the contact value $g(R^+)$, evaluated from the Percus-Yevick hard sphere correlation function. For $g(R^+)$ smaller than 1.05, the analytic approach of section 2.3 is typically sufficient (green). The red areas around $R \approx 12$ nm and $c \approx 1.5$ mM mark infeasible regions, for which the packing fraction exceeds the maximal packing fraction attainable by random close packing (pale red) and by hexagonal/cubic close packing (dark red), respectively.

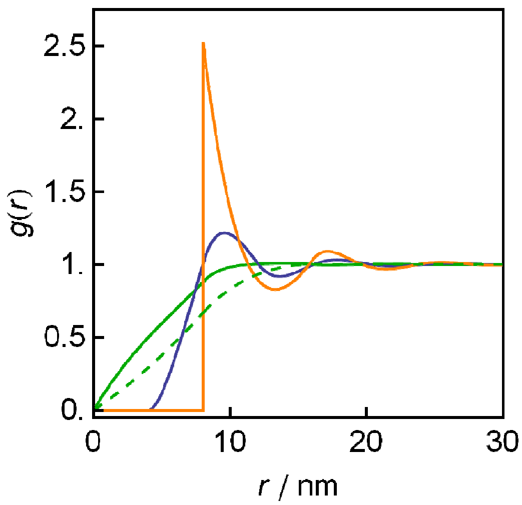

Fig. S2: Pair correlation functions, $g(r)$, of hard-sphere particles labeled at different off-center positions. The radius of the pervaded volume is R = 8 nm and the packing fraction η = 32.3 %. The spins(labels) are attached at the center (orange, $R_1 = R_2 = 0$), at $R_1 = R_2 = R/4$ (blue), and at $R_1 = R_2 = R/2$ (green; surface spin(label)), respectively. For the green dashed curve $\eta = 0$ was assumed, i.e., the pair correlation function $g_c(r)$ of the particle centers equals the Heaviside step function.

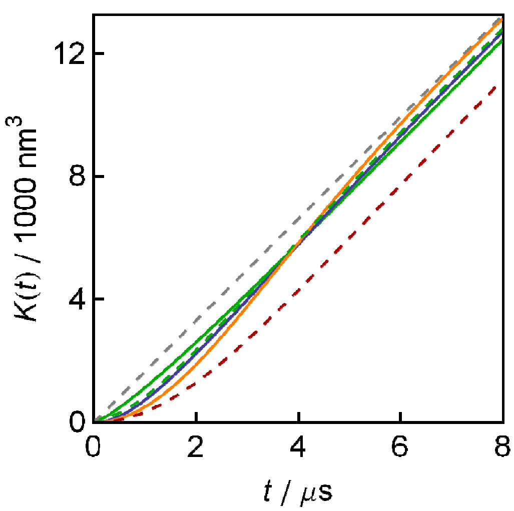

Fig. S3: Decay functions $K(t)$ corresponding to the scenarios given in Fig. S2.The dashed, gray line corresponds to the exponential decay function in the absence of excluded volume effects (eq. (2)). The dashed, red curve gives $K(t)$ evaluated for $R_1 = 0$ and $\eta = 0$, i.e., in the limit that the pair correlation function $g_c(r)$ is given by the Heaviside step function (cf. section 2.3). For more details see Fig. S2.

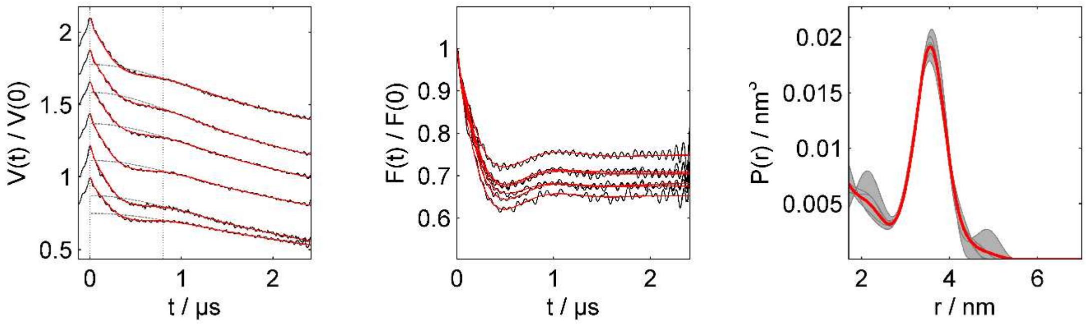

Figure S4: DEER measurements and analysis of 16-DSA doped into HSA (protein-to-probe ratio = 1:2; various protein concentrations ranging from 300 to 700 μM). The DEER time traces have been analyzed one by one using the Tikhonov regularization (α = 250 corresponding to the average value of the optimal αs taken from the *L*-curve) with backgrounds corrected prior to the analysis (background fitted for t > 800 ns; excluded volume effects are accounted for by using eq. (17), R = 5.50 nm). *Left:* Experimental data (black), the non-exponentially decaying background arising from remote spins (gray dashed line), and the fit by the Tikhonov procedure. *Middle:* Normalized, background corrected time traces, $F(t)/F(0)$. Experimental data (black) and the corresponding fits (red) are shown. *Right:* Distance distributions. The individual distance distributions are displayed as gray lines and the weighted average as a red, thick line; the maximal sample-to-sample variance is shown by the gray shaded region.

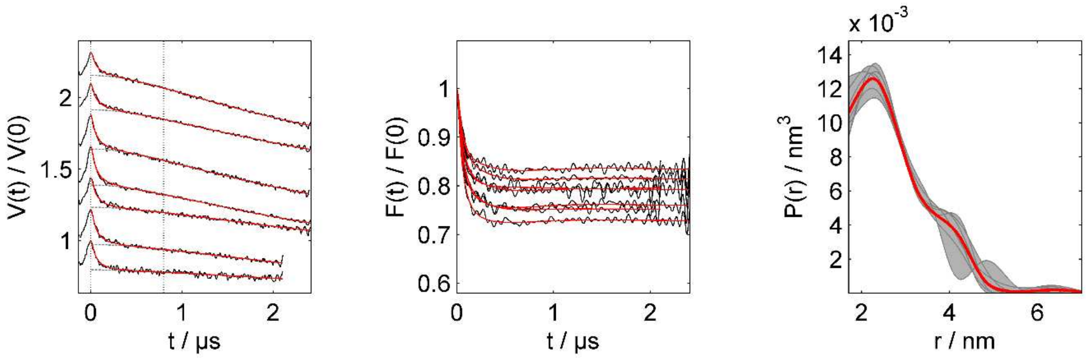

Figure S5: DEER measurements and analysis of 5-DSA doped into HSA (protein-to-probe ratio = 1:2; various protein concentrations ranging from 100 to 600 μM). The DEER time traces have been analyzed individually using the Tikhonov regularization (α = 1000; mild undersmoothing) with backgrounds corrected prior to the analysis (background fitted for t > 800 ns; excluded volume effects are accounted for by using eq. (17), R = 5.25 nm). See Figure S4 above for further details.

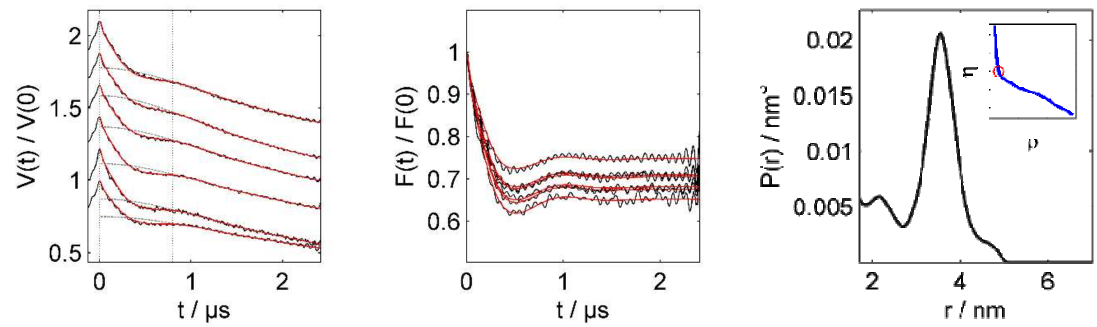

Figure S6: DEER data and results of the simultaneous analysis of 16-DSA doped into HSA (protein-to-probe ratio = 1:2; various protein concentrations ranging from 300 to 700 µM). All DEER time traces have been analyzed at once using a simultaneous Tikhonov regularization procedure with backgrounds corrected prior to the analysis (background fitted for $t > 800$ ns; excluded volume effects are accounted for by using eq. (17), R = 5.50 nm). *Left:* Experimental data (black), the background arising from remote spins (gray dashed line), and the fit by the simultaneous Tikhonov procedure. *Middle:* Background corrected time traces, $F(t)$. Experimental data (black) and the corresponding fits (red) are shown. *Right:* Common distance distribution from the simultaneous Tikhonov regularization (black) and L-curve (blue). The red circle in the L-curve insert indicates the position of the chosen regularization parameter (α = 300). The L-curve is a double logarithmic representation of the weighted square deviation of the experimental form factor from its fit, η, and the square norm of the (discretized) second derivative of $P(r)$ with respect to r, ρ.

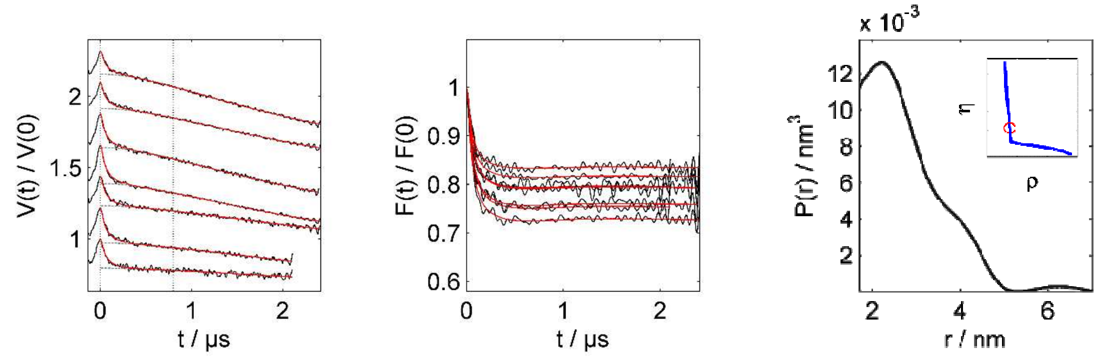

Figure S7: DEER data and results of the simultaneous analysis of 5-DSA doped into HSA (protein-to-probe ratio = 1:2; various protein concentrations ranging from 100 to 600 µM). All DEER time traces have been analyzed at once using a simultaneous Tikhonov regularization procedure with backgrounds corrected prior to the analysis (background fitted for $t > 800$ ns; excluded volume effects are accounted for by using eq. (17), R = 5.25 nm). See Figure S6 above for further details. The regularization parameter (α = 3000) gives rise to mild undersmoothing according to the L-curve criterion.

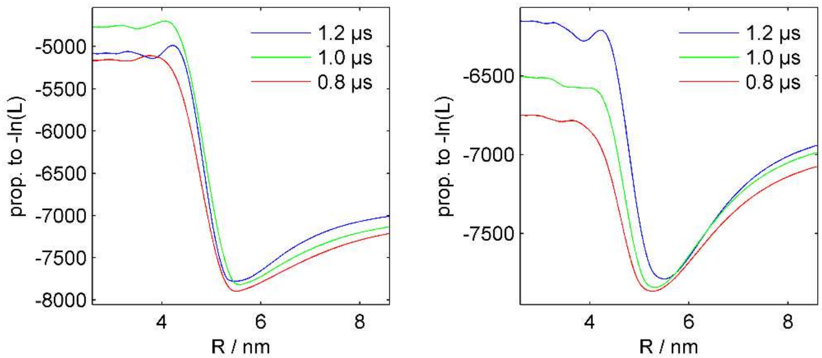

Figure S8: Negative logarithm of the likelihood function *L* (see reference 18 of the main manuscript) of the radius *R* of the covolume, resulting from the simultaneous Tikhonov fitting procedure. The background model was fitted to the original DEER time traces for $t > t_{BG}$ prior to the regularization step (sequential approach). This renders the result parametrically dependent on t_{BG}. The values of t_{BG} are indicated in the figure legend. The most likely *R*s, which correspond to the minima of the curves, are summarized in Table S2.

Table S2: Most likely radii of the pervaded volume resulting from the simultaneous Tikhonov approach with sequential background correction (cf. Figure S8). The errors quoted for *R* are symmetric 95% confidence intervals, evaluated from the posterior probability density of *R*. log(*Q*) is the decadic logarithm of the ratio of the posterior likelihoods of the current and the most likely result among the tested t_{BG}s.

	t_{BG} / µs	*R* / nm	log(*Q*)
16DSA	**1.2**	5.49 ± 0.06	52
6 samples	**1.0**	5.57 ± 0.03	34
	0.8	5.50 ± 0.04	0
5-DSA	**1.2**	5.52 ± 0.06	34
7 samples	**1.0**	5.31 ± 0.05	11
	0.8	5.25 ± 0.06	0

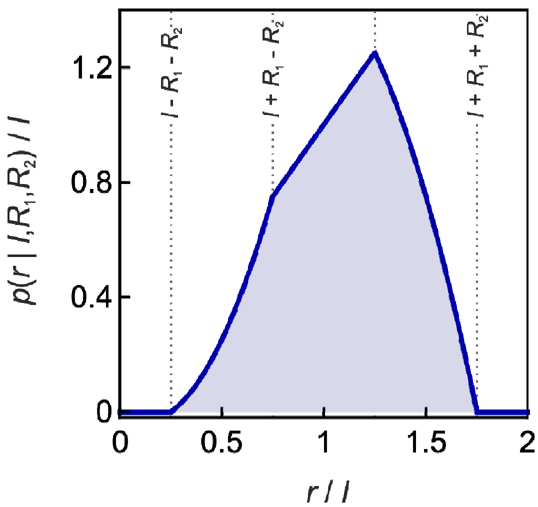

Figure S9: Illustration of the probability density of distances for points distributed on two spheres (one point from each sphere, radii R_1 and R_2, respectively) at distance d, $p(r|d,R_1,R_2)$. See Figure C1 for a schematic. $R_1 = d/4$ and $R_2 = d/2$. The three, non-zero branches are connected at $r = d \pm R_1 \pm R_2$ (dashed, vertical lines).